

# Macromolecular Assemblies of Segmented Poly(ester urethane)s and Poly(ether urethane)s

Silvia Ioan, Mihaela Lupu, Virginia Epure, Aurelia Ioanid, Doina Macocinschi

“Petru Poni” Institute of Macromolecular Chemistry, 700487 – Iasi, Romania

Received 10 November 2005; accepted 1 April 2006

DOI 10.1002/app.24562

Published online 12 October 2007 in Wiley InterScience (www.interscience.wiley.com).

**ABSTRACT:** Polyurethanes containing different soft and hard segments were investigated by fluorescence and scanning electron microscopy. The polarity dependence of the vibrational structure of the pyrene emission spectrum indicated the formation of aggregates at concentrations, which are significantly below the critical concentrations, which define the separation of dilute-semidilute domains. Unlike the samples with 4,4'-methylene diphenylene diisocyanate, the samples with 2,4-tolylene diisocyanate in hard segments

give the fluorescence spectra in which the pyrene excimer appears. The supermolecular structures associated with the form of spherulites or of spherical micelles were detected by scanning electron microscopy. The results were compared with previous reports concerning viscometric data. © 2007 Wiley Periodicals, Inc. *J Appl Polym Sci* 107: 1414–1422, 2008

**Key words:** polyurethanes; fluorescence; electron microscopy; association

## INTRODUCTION

Intermolecular as well as intramolecular association of segmented polyurethanes play an important role in the formation of specific molecular and supermolecular structures in both solid state and solution.<sup>1</sup> In solutions, the urethane groups can interact with each other through various secondary binding forces, classified mainly as hydrogen bonds. The changes observed in solution's properties during ageing can be explained as induced by long-term conformational changes resulting from the intramolecular hydrogen bonding between the urethane groups.<sup>2,3</sup> Also, intramolecular crosslinking of macromolecules during synthesis process is based on a favorable competition between intramolecular reactions, involving the functional groups of a single chain, and an intermolecular reaction between the functional groups of different chains.<sup>4–6</sup> These structures are inclined to form molecular clusters in solution, and their formation and dissociation is in a nonequilibrium state, resulting in a continuous change of the particle size.

The macromolecular assemblies are of considerable interest not only theoretically, but also because of the numerous, promising, potential applications of theirs.<sup>7–9</sup> Techniques such as light scattering, ultracentrifugation, viscometry, osmometry, size-exclusion chromatography, scanning electron microscopy, and others, have resulted in a wealth of data describing many micellar properties, including critical micelle

concentration, the thermodynamics of micelle formation, the equilibrium between micelles and unimers, and the micellar size.<sup>10</sup> Also, steady-state and time-dependent fluorescence and fluorescence depolarization, along with fluorescence quenching experiments, have proven to be valuable tools in expanding the understanding of many micellar properties.<sup>10,11</sup> Excimer fluorescence was used to demonstrate the transition from intra- to intermolecular association, with increase in concentration in dilute solutions. Studies have shown that excimer fluorescence is a highly-suited technique to discriminate intra- from intermolecular associations. Thus, fluorescence measurements provide valuable complementary information to that obtained with other methods, offering the possibility of distinguishing between intra- and interchain interactions.

Previous publications in the field<sup>12–19</sup> presented the syntheses and some properties of a new series of segmented and crosslinked polyurethanes. The influence of polymer structure on thermal stability, the behavior in different organic solvents, the structure and morphology of these compounds were analyzed. The purpose of the present study is to provide additional data on the macromolecular assemblies in poly(ether urethane) and poly(ester urethane), by fluorescence spectra and scanning electron microscopy.

## EXPERIMENTAL

### Structure and compositional parameters of poly(ester urethane)s and poly(ether urethane)s

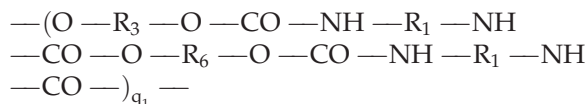
The samples containing segmented block copolyurethanes were prepared by the reaction of aromatic diisocyanates, such as 4,4'-methylene diphenylene diiso-

Correspondence to: S. Ioan (sioan@icmpp.ro).

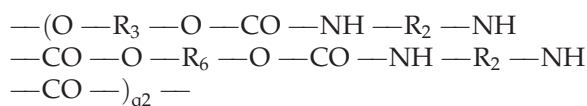
cyanate (MDI) or 2,4-tolylene diisocyanate (TDI), with poly(ethylene glycol)adipate (PEGA), poly(propylene glycol) (PPG) or polytetrahydrofuran (PTHF) and 4,4'-dihydroxydiethoxydiphenyl sulfone (DEDS), thiodiglycol (TDG) or diethylene glycol (DEG) as chain extenders, by applying a two step polyaddition process in *N,N*-dimethylformamide (DMF).<sup>2,16-19</sup>

The general chemical structures are:

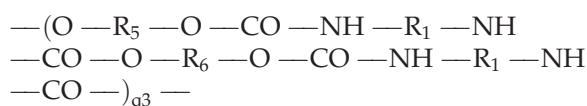
1. PEGA/MDI-DEDS sample:



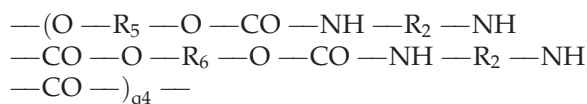
2. PEGA/TDI-DEDS sample:



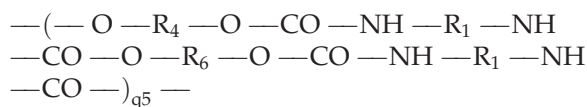
3. PEGA/MDI-DEG sample:



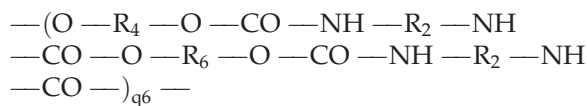
4. PEGA/TDI-DEG sample:



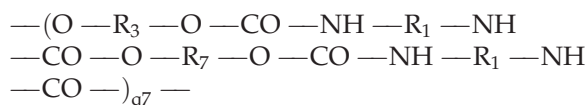
5. PEGA/MDI-TDG sample:



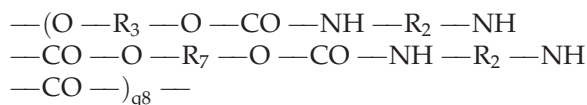
6. PEGA/TDI-TDG sample:



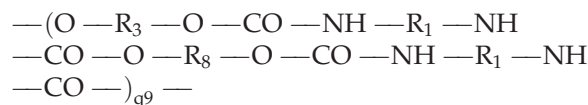
7. PPG/MDI-DEDS sample:



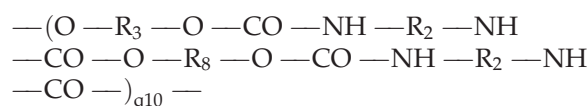
8. PPG/TDI-DEDS sample:



9. PTHF/MDI-DEDS sample:



10. PTHF/TDI-DEDS sample:



where the hard segments are:

R<sub>1</sub> = ---C<sub>6</sub>H<sub>4</sub>---CH<sub>2</sub>---C<sub>6</sub>H<sub>4</sub>--- derived from MDI

R<sub>2</sub> = ---C<sub>6</sub>H<sub>3</sub>(CH<sub>3</sub>)--- derived from TDI

R<sub>3</sub> = ---(CH<sub>2</sub>)<sub>2</sub>---O---C<sub>6</sub>H<sub>4</sub>---SO<sub>2</sub>---C<sub>6</sub>H<sub>4</sub>---O---  
---(CH<sub>2</sub>)<sub>2</sub>--- derived from DEDS

R<sub>4</sub> = ---(CH<sub>2</sub>)<sub>2</sub>---S---(CH<sub>2</sub>)<sub>2</sub>--- derived from TDG

R<sub>5</sub> = ---(CH<sub>2</sub>)<sub>2</sub>---O---(CH<sub>2</sub>)<sub>2</sub>--- derived from DEG

and the soft segments are:

R<sub>6</sub> = [---(CH<sub>2</sub>)<sub>2</sub>O---CO---(CH<sub>2</sub>)<sub>4</sub>---CO---O---]<sub>n</sub>  
---(CH<sub>2</sub>)<sub>2</sub>--- derived from PEGA

R<sub>7</sub> = ---[(CH<sub>2</sub>)<sub>3</sub>---O]<sub>k</sub>--- derived from PPG

R<sub>8</sub> = ---[(CH<sub>2</sub>)<sub>4</sub>---O]<sub>p</sub>--- derived from PTHF

Subscripts "q<sub>1</sub>-q<sub>10</sub>" and "n," "k," "p" represent the polymerization degree.

Table I lists the compositional parameters, number average molecular weight, polydispersity indices, and intrinsic viscosities in DMF for the studied samples.

### Fluorescence spectroscopy

Steady-state fluorescence measurements were carried out with a PerkinElmer spectrometer LS 55. For fluorescence measurements, 3.5 mL of solution was placed in a 1.0 cm square quartz cell.

Stock solutions of pyrene (Kodak, purified by twice repeated recrystallization from methanol) with a final concentration of 7.9 × 10<sup>-6</sup> M were prepared in DMF from a small amount of pyrene solution in methanol. Methanol was not removed, its final content being of 0.1/200 v/v. Probe concentrations in the prepared samples were estimated from UV spectra.

Polyurethane solutions with concentrations between 0.004 and 2.66 g/dL were prepared by the dissolution

TABLE I  
Compositional Parameters of Soft and Hard Segments, Number Average Molecular Weights,  $M_n$ , Polydispersity Indices,  $M_w/M_n$ , and Intrinsic Viscosities

Sample	Weight ratio (%) $R_{6,7, \text{ or } 8} : (R_1 \text{ or } 2 : R_{3,4, \text{ or } 5})$	$M_n$	$M_w/M_n$	$[\eta]$ , dL/g, DMF, 25°C
PEGA/MDI-DEDS	69.26 : (18.33 : 12.41)	28,000	1.56	0.474
PEGA/TDI-DEDS	73.18 : (13.57 : 13.25)	25,900	1.55	0.210
PEGA/MDI-DEG	75.43 : (16.36 : 8.21)	20,800	1.77	0.399
PEGA/TDI-DEG	80.11 : (13.24 : 6.65)	20,100	1.67	0.187
PEGA/MDI-TDG	74.98 : (16.67 : 8.35)	22,300	1.83	0.475
PEGA/TDI-TDG	79.59 : (13.59 : 6.82)	18,800	1.53	0.219
PPG/MDI-DEDS	69.26 : (18.33 : 12.41)	29,300	1.33	0.217
PPG/TDI-DEDS	73.18 : (13.57 : 13.25)	20,200	1.28	0.183
PTHF/MDI-DEDS	69.26 : (18.33 : 12.41)	39,200	1.38	0.430
PTHF/TDI-DEDS	73.18 : (13.57 : 13.25)	37,100	1.39	0.338

of appropriate amounts copolymer in 5 mL of pyrene-DMF solution, and left for 24 h at room temperature, heated 20 min at 50°C and left again to equilibrate before measurements.

For emission spectra,  $\lambda_{\text{ex}}$  was 335 nm, and for excitation spectra,  $\lambda_{\text{em}}$  was 394 nm. Excitation and emission spectra were measured in the 300–360 nm and 350–500 nm ranges, respectively, for identical sample volumes.

To verify the nature of the excimer, which appears in some fluorescence spectra, the emission wavelength was set at 374 and 443 nm. The ratio between excimer emission intensity and monomer emission intensity ( $I_{\text{ex}}/I_m$ ) was calculated by dividing intensity at 443 nm to that at 374 nm. The excitation and emission bandwidths were of 8 and 4 nm, respectively. All measurements were performed at room temperature, using air-equilibrated solutions.

### Scanning electron microscopy

The macroscopic morphological feature was investigated by scanning electron microscopy (SEM), operating at 20 kV, with secondary electrons with a TESLA BS 301. The studies were performed on untreated polyurethane films and treated polyurethane films in low pressure plasma performed on an installation having the following characteristics: intensity, 3000 V/cm; frequency, 1.3 MHz; pressure, 0.58 mbarr, and duration, 10 min. The polyurethane samples were dissolved in DMF and cast from the solution (1 g/dL) onto glass plates. The DMF evaporated slowly at room temperature, the films were completely dried in vacuum and then covered with a thin layer of carbon-gold.

## RESULTS AND DISCUSSION

### Fluorescence spectra of pyrene in polyurethane solutions

The association of polyurethanes from Table I in DMF solutions was examined by fluorescence technique,

using pyrene as a probe. This method is based on the sensitivity of the probe to the hydrophobicity and polarity of its microenvironment.<sup>20–22</sup> In the presence of micelles or similar supramolecular aggregates, pyrene is solubilized inside the hydrophobic part of such aggregates. As a result, significant changes in the spectroscopic properties are observed upon transfer of the probe from solvent environment to the nonpolar environment of the polymer. Such changes are exemplified in Figure 1, which presents typical excitation and emission spectra recorded for pyrene in the DMF solutions of PEGA/MDI-DEDS, at various concentrations.  $I_1$  peak, which arises from the (0,0) transition from the lowest excited electronic state, is a “symmetry-forbidden” transition that can be enhanced by the distortion of the  $\pi$  electron cloud. Thus,  $I_1$ , occurring at  $\lambda = 374$  nm yields enhanced the values of fluorescence intensity in the polar solvent DMF. On the other hand, peak  $I_3$  (at approximately 385 nm) is not forbidden and thus it is relatively insensitive to DMF polarity. Similar spectra were obtained for all samples with MDI in hard segments.

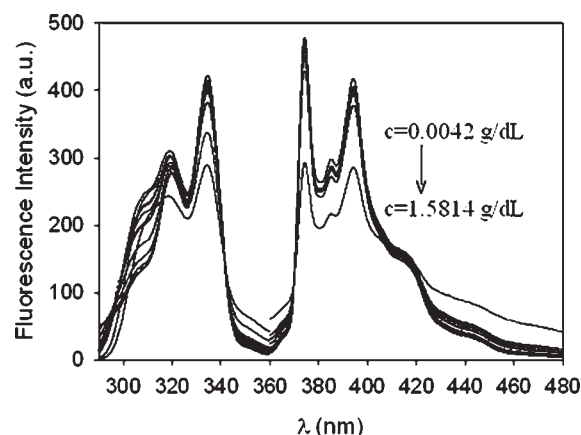
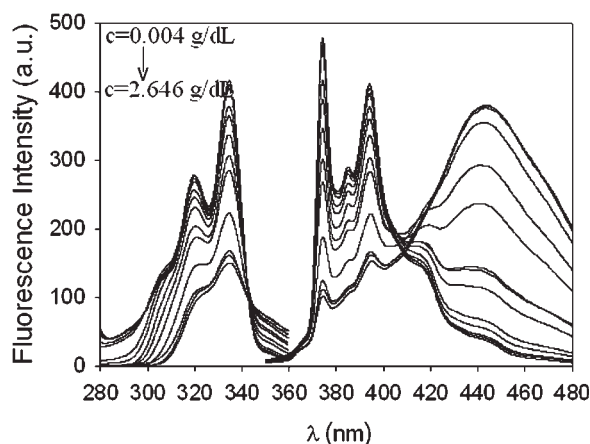


Figure 1 Fluorescence excitation and emission spectra of PEGA/MDI-DEDS recorded at various concentrations in DMF at room temperature.



**Figure 2** Fluorescence excitation and emission spectra of PEGA/TDI-TDG recorded at various concentrations in DMF at room temperature.

Surprisingly, for samples with TDI in the hard segments, pyrene excimer formation was detected. For samples with MDI in the hard segment, the fluorescence spectra show that the excimer formation is a minor process due to the higher rigidity of the chain.<sup>23,24</sup>

Literature shows that the formation of a pyrene excimer requires encounter of an electronically excited pyrene with a second pyrene in its ground electronic state ("dynamic" excimer:  $M^* + M = E^*$ ) or of a pre-associated pyrene dimer in the ground-state ("static" excimer:  $M - M = D \rightarrow D^*$ ).<sup>25</sup> The structureless emission band from 440 to 650 nm is attributed to the pyrene excimer.<sup>26</sup>

Literature reported cases of "static" pyrene excimer when chromophore in free state was used.<sup>27</sup> At the same concentration of pyrene solution ( $7.9 \times 10^{-6}$  M),

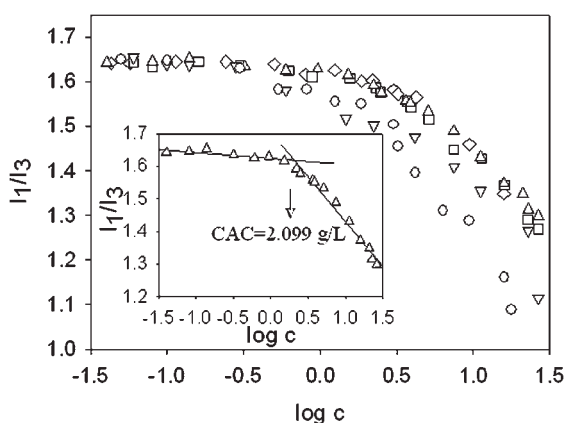


**Figure 3** Fluorescence intensity ratio  $I_1/I_3$  (from pyrene emission spectra) as a function of concentration (g/L) for PEGA/MDI-DEDS ( $\diamond$ ), PEGA/MDI-DEG ( $\square$ ), PEGA/MDI-TDG ( $\triangle$ ), PPG/MDI-DEDS ( $\nabla$ ) and PTHF/MDI-DEDS ( $\circ$ ) in DMF. The small plot exemplifies CAC determination for the PEGA/MDI-TDG sample.

for the copolymers with TDI hard segment, the formation of excimer was observed. When polymer's concentration is increased, a new broad band appears, with maximum at 443 nm. This peak is assigned to the excimer emission.

As a typical example, Figure 2 presents the emission of pyrene with the (0,0) band at 374 nm and a broad excimer emission at 443 nm of PEGA/TDI-TDG ( $\lambda_{ex} = 335$  nm).

### Critical aggregation concentration from fluorescence spectra

It has to be noted that determination of a true onset of aggregation is a rather delicate problem. In DMF, which is a polar solvent, aggregation takes place, leading to the formation of micelles. The micelles consist in a core of the insoluble or less soluble hard segments, surrounded by flexible segments (corona). The formation of copolymer micelles in organic solvents is an enthalpy-driven process, whereas micelle formation in aqueous systems is considered as an entropic-driven process.<sup>28</sup> When using a free probe, location of the pyrene is not exactly known; it can be located in the more hydrophobic domains or in a range of sites with varying distance to the copolymer. Ratio  $I_1/I_3$  of the intensities of the first to the third peak is an index of the polarity of pyrene environment.<sup>11,22</sup> The sensitivity of this ratio in several solvent were tabulated in literature.<sup>29,30</sup> These values range from 1.8 to 1.9 in water, to 0.95 for polystyrene films, and to about 0.5 for nonpolar solvents such as hexane, being thus very helpful for determining the location of the pyrene probe in the micelles.

In the present work, two different methods were used to obtain critical aggregation concentration val-

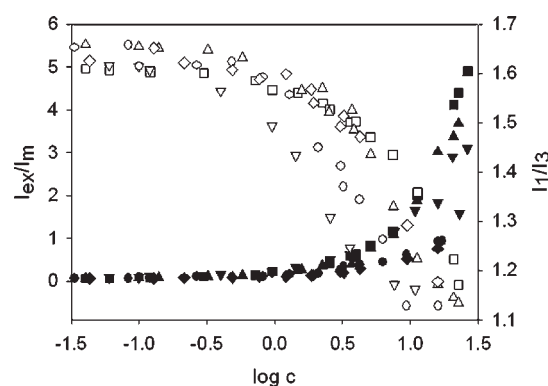


**Figure 4** Ratio of excimer emission intensity to monomer emission intensity,  $I_{ex}/I_m$  (black symbols) and the fluorescence intensity ratio  $I_1/I_3$  (white symbols) as a function of polyurethane concentrations (g/L) in DMF: ( $\blacklozenge$ ,  $\diamond$ )—PEGA/TDI-DEDS; ( $\blacksquare$ ,  $\square$ )—PEGA/TDI-DEG; ( $\blacktriangle$ ,  $\triangle$ )—PEGA/TDI-TDG; ( $\blacktriangledown$ ,  $\triangledown$ )—PPG/TDI-DEDS; ( $\bullet$ ,  $\circ$ )—PTHF/TDI-DEDS.

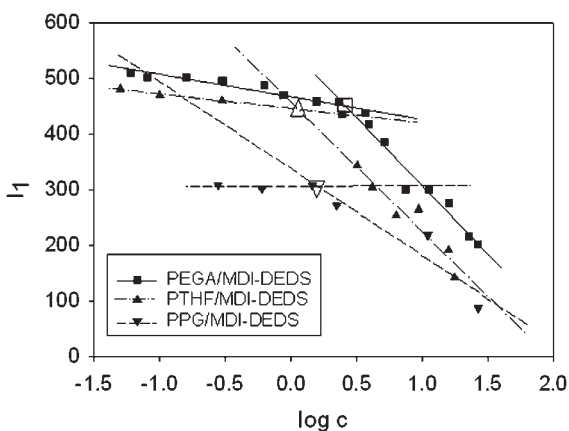


**Figure 5** Dependence of fluorescence intensity  $I_1$  (from pyrene emission spectra) on concentration, for PEGA/MDI-DEDS, PTHF/MDI-DEDS, PPG/MDI-DEDS (g/L) in DMF. Black symbols are the experimental data and white symbols are the CAC values.

ues (CAC) from the fluorescence spectra. These values were determined from the concentration dependence of the fluorescence intensity ratio  $I_1/I_3$  (Fig. 3—for samples with MDI in the hard segment, and Fig. 4, respectively,—for samples with TDI in the hard segment) or of the fluorescence intensity  $I_1$  (Fig. 5—for samples with MDI-DEDS in the hard segment) by a simple procedure involving crossover points in the studied concentration ranges. For pyrene solutions in DMF without any polyurethane added,  $I_1/I_3$  takes a value of 1.6. For the studied polyurethanes, at the lowest concentration at which measurements were made,  $I_1/I_3$  has a value of 1.65, which is slightly higher than the value of 1.6. A minimum value of  $\cong 1.1$  at a polyurethane concentration around to 0.20 g/dL indicates the complete transfer of pyrene molecules from the solvent to the hydrophobic environment of the polyurethanes with MDI and TDI in the hard segment. At lowest polyurethanes concentrations, a plateau value of the polarity ratio is reached. As polyurethane concentrations are increased, more aggregation is to be observed, and more of the probe resides in the hydro-

phobic domains, which results in a decrease of the  $I_1/I_3$  ratio. The shape of the curve  $I_1/I_3$  versus concentration indicates that the signal change in the region of a certain concentration can be related to the CAC values.

Generally, it is assumed that in polar solvents, the hydrophilic groups are in a good solvent, while hydrophobic groups are in poor solvent, so that they tend to aggregate.<sup>31</sup> A critical aggregation concentration was observed for all studied samples, however at higher concentrations for poly(ester urethane)s, than those for poly(ether urethane)s, according to data presented in Table II. These results are confirmed by a higher quality of solvent for PEGA than for PPG or PTHF according to the solubility parameters from Table III.

These concentration values are much smaller than the overlap concentration,  $c^*$ , estimated from intrinsic viscosity ( $c^* \cong [\eta]^{-1}$ , Table II) indicating that hydrophobic interactions exist even in dilute solutions.

### Excimer formation

For polyurethanes with TDI in their hard segments, excimer appearance can be used as a parameter indicating the changes in the conformation and flexibility of the macromolecular chains. Figure 4 is a best illustration of the variation  $I_{ex}/I_m$  with the increase of polyurethanes concentration. Below a certain concentration, the intensity emitted by the excimer is very low and nearly constant ( $I_{ex}/I_m \cong 0.1$ , suggesting polymer coil expansion and/or rigidity, whereas a large value of  $I_{ex}/I_m$  suggests polymer chain contraction and/or high segmental mobility. When the polymer concentration increases, the locally excited state emission ( $I_m$ ) is actually observed to decrease, while the excimer emission ( $I_{ex}$ ) increases, which agrees with system transition from intra- to intermolecular association.<sup>32</sup> Principally, pyrene excimers can be formed from pyrenes within one polymer (intrapolymeric), or from pyrenes, on different polymers (interpolymeric association). It is very difficult to distinguish from intra- and intermolecular polymer association based only on

**TABLE II**  
Critical Aggregation Concentrations and Critical Concentrations Between the Dilute–Semidilute Domains for Polyurethanes

Samples	CAC, g/dL (from $I_1/I_3$ )	CAC, g/dL (from $I_1$ )	$c^*$ (g/dL)
PEGA/MDI-DEDS	0.267	0.264	2.110
PEGA/TDI-DEDS	0.242	0.229	4.762
PEGA/MDI-DEG	0.224	0.264	2.506
PEGA/TDI-DEG	0.240	0.209	5.348
PEGA/MDI-TDG	0.210	0.333	2.105
PEGA/TDI-TDG	0.236	0.197	4.783
PPG/MDI-DEDS	0.119	0.159	4.608
PPG/TDI-DEDS	0.097	0.125	5.464
PTHF/MDI-DEDS	0.143	0.113	2.326
PTHF/TDI-DEDS	0.088	0.129	2.958

TABLE III  
Solubility Parameters  $\delta_1$  and  $\delta_2$  from the Theoretical Data Calculated with Cohesive Energy,  $E_{\text{coh}(1)}$  or  $E_{\text{coh}(2)}$  and Molar Volume,  $V$ , for the Soft and Hard Segments of the Studied Polyurethanes

Soft and hard segments of polyurethanes	$E_{\text{coh}(1)}$ ( $10^{-5}$ ) (J/mole)	$E_{\text{coh}(2)}$ ( $10^{-5}$ ) (J/mole)	$V$ (298 K) (cc/mole)	$\delta_1$ ( $\sqrt{\text{J/cc}}$ )	$\delta_2$ ( $\sqrt{\text{J/cc}}$ )
PEGA	0.644	0.500	136.64	21.08	19.12
PPG	0.180	0.188	55.15	18.05	18.48
PTHF	0.229	0.234	71.24	17.24	18.11
MDI-DEDS	3.623	5.950	568.93	25.23	32.34
MDI-DEG	2.656	4.145	453.62	24.20	30.23
MDI-TDG	2.760	4.099	469.58	24.24	29.54
TDI-DEDS	3.022	5.502	451.83	25.86	34.90
TDI-DEG	2.055	3.710	337.63	24.67	33.15
TDI-TDG	2.160	3.664	353.59	24.71	32.19

pyrene fluorescence. However, if these species are in dynamic equilibrium, dilution of the polymer solution will minimize interpolymeric association, leading to a decrease of the  $I_{\text{ex}}/I_m$  ratio. Figure 4 plots graphically the decrease of  $I_{\text{ex}}/I_m$  with decreasing polyurethane concentrations, showing a dynamic equilibrium of the system. The value of concentration at intersection of the tangents to the portions of the curve  $I_{\text{ex}}/I_m$  versus concentration is slightly higher than the CAC value determined in Figure 4 from the curve  $I_1/I_3$  versus concentration.

For identifying the excimer nature, the normalized excitation spectra of PEGA/TDI-DEDS and PTHF/TDI-DEDS solutions to the intensity of monomer emission ( $\lambda = 374$  nm) and to the intensity of excimer emission ( $\lambda = 443$  nm) were plotted in Figure 6.

Differences were observed between the excitation spectra obtained at the wavelength of the monomer and the excimer emissions.

Excimer emission of pyrene-labeled polymers can arise via a dynamic process or via preassociated pyrenes.<sup>33</sup> In the former case, the incident light excites isolated pyrene groups, which then diffuse and encounter a ground-state pyrene to form an excimer. "Static excimer" is formed by direct excitation of pyrene dimers or aggregates. These processes of excimer formation exhibit different excitation spectra, and thus one can distinguish: dynamic excimers, with excitation spectra identical to that of monomer emission; when associated pyrene groups are present, the spectrum monitored at excimer emission is red-shifted, compared to the one obtained for the monomer. It is very difficult to know from steady-state measurements if the pyrene excimer is "static" or "dynamic." The formation of "dynamic" or "static" pyrene excimers on polymer depends on many factors, of which hydrophobic association of the pyrene groups can be a major contributor.<sup>33</sup> It seems that the red-shift observed in Figure 6 signifies the "static" pyrene excimers due to the preassociation phenomena of pyrene molecules.

### Viscometric results

Generally, the hydrophobic groups affect intrinsic viscosity and Huggins constant ( $k'$ ). Higher values of the Huggins constant are usually interpreted as enhanced polymer-polymer interactions, indicating poorer solvent quality. The tendency of Huggins constant to increase with increasing the hydrophobic content

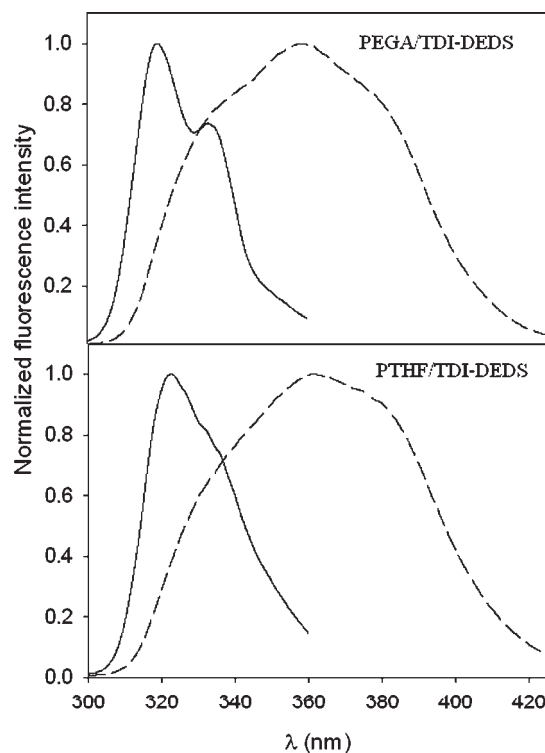
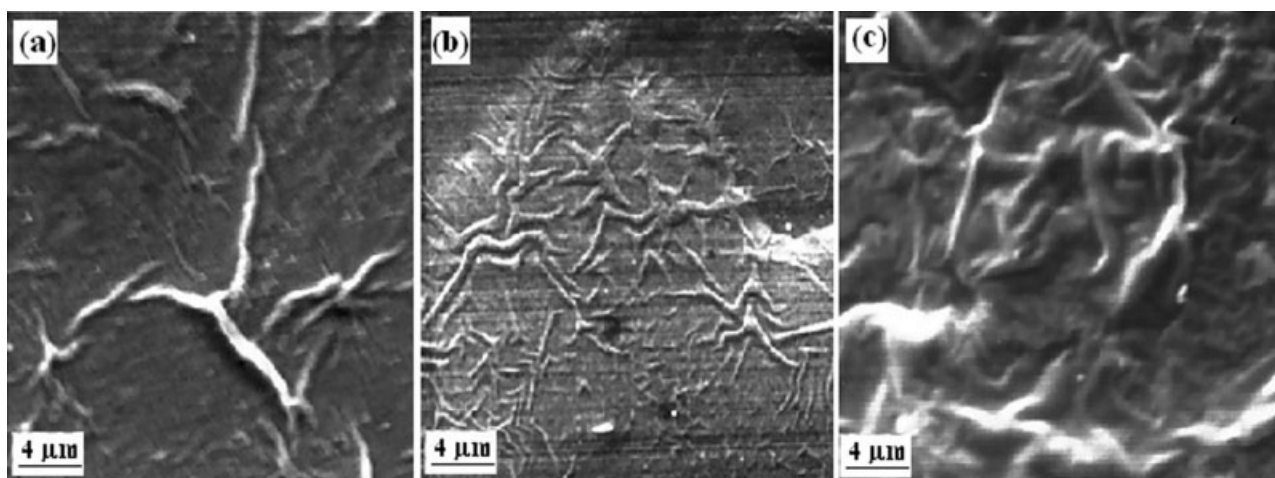


Figure 6 Normalized fluorescence intensity for PEGA/TDI-DEDS solution at  $c = 2.223$  g/dL, and PTHF/TDI-DEDS at  $c = 2.142$  g/dL. The solid line corresponds to the intensity of excitation spectra divided to the intensity of monomer emission ( $\lambda = 374$  nm), and the dashed line corresponds to the intensity of excitation spectra divided to intensity excimer emission ( $\lambda = 443$  nm). The excimer excitation spectrum is red-shifted compared to the monomer excitation spectrum.



**Figure 7** Electron micrographs of the plasma-treated PEGA/MDI-DEDS (a), PPG/MDI-DEDS (b) and PTHF/MDI-DEDS (c) samples.

reflects the possibility of intermolecular association.<sup>34</sup> Previous papers discussed the intrinsic viscosity of these polymers at different temperatures.<sup>2,18,35</sup> The Huggins constants,  $k'$ , for poly(ester urethane)s take mean values of 0.52, slightly higher than the normal value. For poly(ether urethane)s, higher values were obtained, and the correct extrapolation of Huggins equation for obtaining the intrinsic viscosity was affected by errors. We believe that poly(ether urethane)s tend to form different mechanical aggregates in solution, and that the formation and dissociation of molecular clusters is in a nonequilibrium state, which could be a unique behavior of the solutions of cross-linked macromolecules. Moreover, the synthesis process can develop inter- and intramolecular crosslinked structures. The formation of intramolecularly cross-linked macromolecules is based on a favorable competition between intramolecular reactions, involving functional groups of a single chain, and intermolecu-

lar reactions between the functional groups of different chains.<sup>35</sup>

Literature shows that the micelles are formed when block copolymers are dissolved in a selective solvent or solvent mixture and when they are typically composed of two distinct regions: a compact micellar core, consisting of small soluble blocks and an outer shell, or corona, formed of the solvated segments of the soluble blocks. The association number increases with the solvent's selectivity.<sup>36,37</sup> The selectivity of the solvent for polyurethanes was evaluated from the solubility parameters,  $\delta$ , of the soft and hard segments. These parameters were calculated from the theoretical data obtained for cohesive energy,  $E_{coh}$ , and molar volume,  $V$ , according to eq. (1):<sup>38,39</sup>

$$\delta_{1,2}(298 \text{ K}) = \sqrt{E_{coh1,2}/V(298 \text{ K})} \quad (1)$$

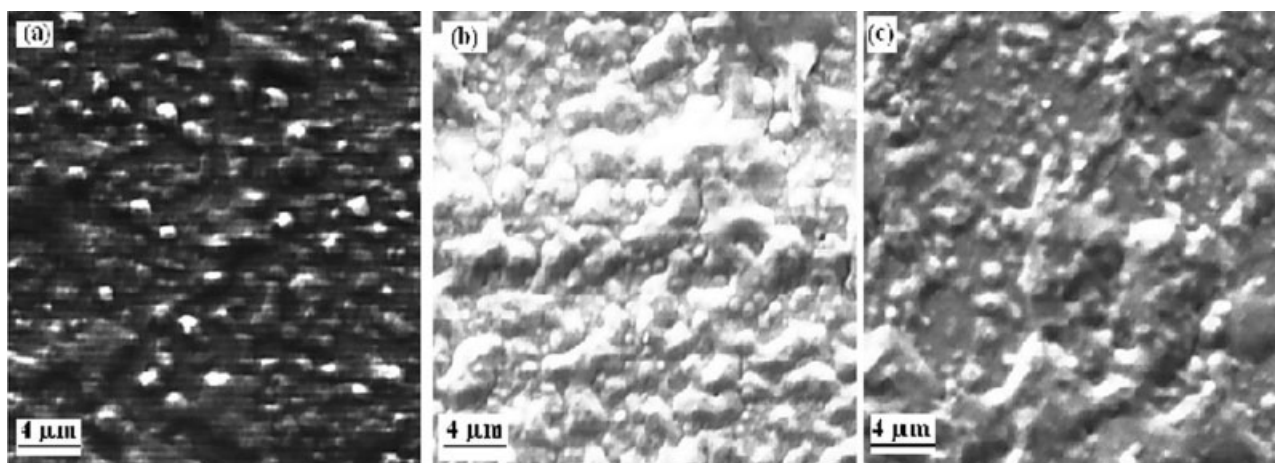


**Figure 8** Electron micrographs of the plasma-treated PEGA/TDI-DEDS (a), PPG/TDI-DEDS (b) and PTHF/TDI-DEDS (c) samples.

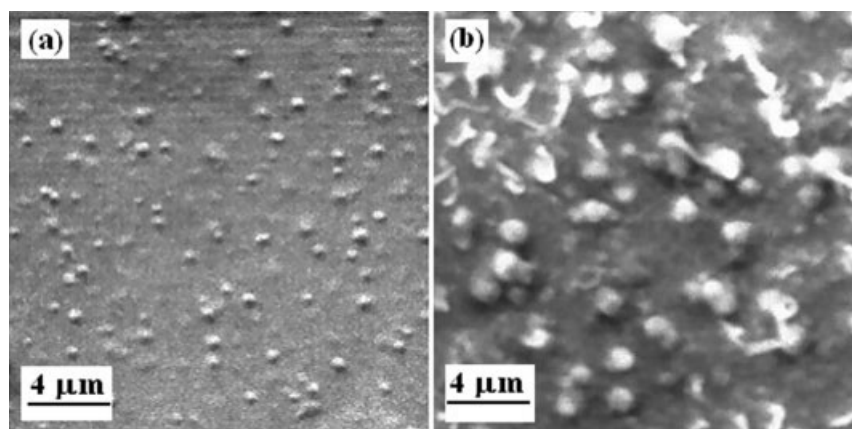


**Figure 9** Electron micrographs of the untreated (a) and plasma-treated (b) PEGA/TDI-TDG sample.

Subscripts "1" and "2" represent the two different correlations for  $E_{\text{coh}}$ , which employ the group contributions of Fedors and van Krevelen-Hofter, respectively.

Table III shows that DMF with  $\delta = 24.7$  is a better solvent for hard segments (MDI-DEDS, MDI-DEG, MDI-TDG, TDI-DEDS, TDI-DEG, or TDI-TDG) than for soft segments (PEGA, PPG, or PTHF).

The presence of the polarity and/or of the hydrogen bonding may have significant effects on the dissolution of polyurethanes, so that the "core" and "corona" formations of micelles are difficult to be discussed. Literature shows that solubility depends on the hard block length and concentration and, to a lesser extent, on the nature of the soft segment. Specific properties of polyurethane solutions may arise from the possible structure formation, as due to the association of macromolecules and rigid hard blocks.<sup>1</sup>

### Supermolecular structures of polyurethanes by SEM

The morphology of these polyurethanes is very complicated not only because of their two-phase structure, but also because of physical phenomena such as crystallization and hydrogen bonding. Literature shows that a rod-like or lamellar structure appears for a hard segment composition of 42–67% and that the hard segment phase is dispersed in the matrix of the soft segments in the form of either short cylinders or spherulites, for hard segment composition less than 31%.<sup>40</sup>

Figures 7 and 8 show the electron micrographs of the poly(ester urethanes) and poly(ether urethanes) with MDI-DEDS and TDI-DEDS in hard segments, in which the solid films were treated in low-pressure plasma. Thus, a better image of the macromolecular texture of polyurethane films was obtained by air plasma treatment, according to the example presented in Figure 9. In this process, bombardment of the polymer surface with energetic particles (electrons, ions,

and free radicals) and UV radiation breaks the covalent bonds of the polymer backbone, resulting in lower molecular weight polymer chains eliminated by a vacuum pump.

From the micrograph of the samples, the two-phase structure is clearly demonstrated; however, the shape of the structural formations depends on the diisocyanate structures. Large supermolecular structures, in the form of spherulites observed at samples with MDI in hard segments, are associated with polyurethanes crystallization. The methyl substituent from TDI can seriously disrupt the symmetry and crystallizability of the diisocyanates, so that the presence of spherical aggregates appears in the micrograph of polyurethanes with TDI. Also, the fluorescence spectra for these samples present excimer formation. Moreover, the higher density of the crystal nuclei was observed at poly(ether urethane)s, comparatively with poly(ester urethane)s. This difference is more visible in studies on solutions of poly(ether urethane)s, when the viscometric data are affected by the serious errors.

### CONCLUSIONS

Fluorescence measurements combined with viscometry and scanning electron microscopy have been used to study aggregate/micelle formation in polyurethanes with different soft and hard segments.

Fluorescence spectra in the DMF solutions of the studied polyurethanes show the existence of hydrophobic aggregates even in dilute solutions, so that the critical aggregation concentrations observed for all studied samples are much smaller than the overlap concentration,  $c^*$ , estimated from intrinsic viscosity. Also, the CAC values are higher for poly(ester urethane)s than those for poly(ether urethane)s.

For samples with TDI in the hard segments, the pyrene excimer formation via a static process was detected.



Large supermolecular structures, associated with crystallization of the polyurethane segments in the form of spherulites, were observed at samples with MDI in the hard segments. Furthermore, a higher density of crystal nuclei was observed at poly(ether urethane)s, comparatively with poly(ester urethane)s. In the micrograph of polyurethanes with TDI, spherical aggregates appear, due to the methyl substituent which can seriously disrupt the symmetry and crystallizability of the diisocyanates.

The obtained results have been compared with our previous data on the associative behavior of polyurethanes in solution. The obtained Huggins constants,  $k'$ , for poly(ether urethane)s, were higher than for poly(ester urethane)s, so that the correct extrapolation of Huggins equation for obtaining intrinsic viscosity was affected by errors, indicating the presence of aggregates in nonequilibrium state. Moreover, the synthesis process can develop inter- and intramolecular cross-linked structures, as observed in the SEM micrographs.

## References

- Petrovic, Z. S.; Ferguson, J. *Prog Polym Sci* 1991, 16, 695.
- Ioan, S.; Lupu, M.; Macocinschi, D. *High Perform Polym* 2003, 15, 319.
- Sivadasan, K.; Somasundaran, P. *J Polym Sci, Part A: Polym Chem* 1991, 29, 911.
- Frank, R. S.; Downey, J. S.; Yu, K.; Stöver, H. D. H. *Macromolecules* 2002, 35, 2728.
- Li, F.; Zuo, J.; Song, D.; Li, Y.; Ding, L.; An, Y.; Wei, P.; Ma, J. B.; He, B. *Eur Polym J* 2001, 37, 193.
- Li, F.; Lu, Z.; Qian, H.; Rui, J.; Chen, S.; Jiang, P.; An, Y.; Mi, H. *Macromolecules* 2004, 37, 764.
- Finningan, B.; Martin, D.; Halley, P.; Truss, R.; Campbell, K. *Polymer* 2004, 45, 2249.
- Pattanayak, A.; Jana, S. C. *Polymer* 2005, 46, 3275.
- Pattanayak, A.; Jana, S. C. *Polymer* 2005, 46, 3394.
- Pergushov, D. V.; Remizova, E. V.; Gradzielski, M.; Lindner, P.; Feldthusen, J.; Zezin, A. B.; Müller, A. H. E.; Kabanov, V. A. *Polymer* 2004, 45, 367.
- Nomura, S.; Cooper, S. L. *Macromolecules* 2000, 33, 6402.
- Ioan, S.; Grigorescu, G.; Stanciu, A. *J Opt Adv Mater* 2000, 2, 397.
- Ioan, S.; Aberle, C. E.; Grigorescu, G.; Stanciu, A.; Aberle, T. *Int J Polym Anal Char* 2002, 7, 210.
- Ioan, S.; Grigorescu, G.; Stanciu, A. *Polymer* 2000, 42, 3633.
- Ioan, S.; Grigorescu, G.; Stanciu, A. *Eur Polym J* 2002, 38, 2295.
- Ioan, S.; Macocinschi, D.; Lupu, M. *Polym Plast Technol Eng* 2004, 43, 491.
- Ioan, S.; Lupu, M.; Taranu, A.; Macocinschi, D. *Int J Polym Mater* 2005, 54, 589.
- Macocinschi, D.; Ioan, S.; Lupu, M.; Grigoras, C. *Mol Cryst Liq Cryst* 2004, 416, 183.
- Grigoriu, A.; Macocinschi, D.; Filip, D.; Vlad, S. *Bull Inst Polit Iasi (Romania), Ser Text* 2001, 47, 109.
- Pinteala, M.; Epure, V.; Harabagiu, V.; Simionescu, B. C.; Schlick, S. *Macromolecules* 2004, 37, 4623.
- Lee, S.; Chang, Y.; Yoon, J. S.; Kim, C.; Kwon, I.; Kim, Y. H.; Jeong, S. *Macromolecules* 1999, 32, 1847.
- Lysenko, E. A.; Bronich, T. K.; Slonkina, E. V.; Eisenberg, A.; Kabanov, V. A.; Kabanov, A. V. *Macromolecules* 2002, 35, 6351.
- Inai, Y.; Sisido, M.; Imanishi, Y. *J Phys Chem* 1990, 94, 8365.
- Ioan, S.; Lupu, M.; Macocinschi, D. *High Perform Polym* 2005, 17, 533.
- Birks, J. B. *Rep Prog Phys* 1975, 38, 903.
- Granville, M.; Jerome, R. J.; Teyssie, P.; De Schryver, F. C. *Macromolecules* 1988, 21, 2894.
- Religio, P.; Martinho, J. M. G.; Farinha, J. P. S. *Macromolecules* 2005, 38, 10799.
- Riess, G. *Prog Polym Sci* 2003, 28, 1107.
- Kalyanasundaram, K.; Thomas, J. K. *J Am Chem Soc* 1977, 99, 2039.
- Dong, D. C.; Winnik, M. A. *Can J Chem* 1984, 62, 2560.
- Vasilievskaya, V. V.; Khalatur, P. G.; Khokhlov, A. R. *Macromolecules* 2003, 36, 10103.
- Wilhem, M.; Zhao, C. L.; Wang, Y.; Xu, R.; Winnik, A. M.; Mura, J. L.; Riess, G.; Croucher, M. D. *Macromolecules* 1991, 24, 1033.
- Winnik, M. A.; Bystryak, S.M.; Liu, Z.; Siddiqui, J. *Macromolecules* 1998, 31, 6855.
- Desbrieres, J. *Polymer* 2004, 45, 3285.
- Ioan, S.; Macocinschi, D.; Lupu, M. In *New trends in Natural and Synthetic Polymer Science*; Vasile, C.; Zaikov, G. E., Eds.; Nova Science Publishers: New York, 2006; Chapter 13.
- Prochazka, K.; Kiserow, D.; Ramireddy, C.; Tuzar, Z.; Munk, P.; Webber, S. E. *Macromolecules* 1992, 25, 454.
- Zhong, X. F.; Varshney, K.; Eisenberg, A. *Macromolecules* 1992, 25, 7160.
- Bicerano, J. *J Macromol Sci Rev Macromol Chem Phys* 1996, 36C, 161.
- Lupu, M.; Macocinschi, D.; Ioanid, G.; Ioan, S. *Polym Int* 2007, 56, 389.
- Wang, F. Ph.D. Thesis, Faculty of the Virginia Polytechnic Institute, Blacksburg, Virginia, 1998.